SCIENCE CHINA
Information Sciences

• LETTER •

April 2025, Vol. 68, Iss. 4, 149401:1–149401:2
https://doi.org/10.1007/s11432-024-4302-0

High linearity GaN HEMT by optimized three-dimensional-gated modulation via top-MIS-gate nanowire channel structure

Can GONG[1], Minhan MI[1*], Yuwei ZHOU[1], Pengfei WANG[1], Hanzhen LI[1], Xinyi WEN[1], Ting MENG[1], Sirui AN[1], Xiang DU[1], Kai CHENG[2], Meng ZHANG[1], Qing ZHU[1], Xiaohua MA[1] & Yue HAO[1]

[1]*State Key Discipline Laboratory of Wide Band Gap Semiconductor Technology, Xidian University, Xi'an 710071, China*
[2]*Enkris Semiconductor Inc., Suzhou 215123, China*

Received 14 June 2024/Revised 13 August 2024/Accepted 10 February 2025/Published online 6 March 2025

Citation Gong C, Mi M H, Zhou Y W, et al. High linearity GaN HEMT by optimized three-dimensional-gated modulation via top-MIS-gate nanowire channel structure. Sci China Inf Sci, 2025, 68(4): 149401, https://doi.org/10.1007/s11432-024-4302-0

GaN-based high-electron-mobility transistors (HEMTs) have found extensive applications in defense, aerospace, and civilian communications [1, 2]. However, with the increase of gate voltage (V_{GS}), the transconductance (G_{m}) of the device exhibits a decline after reaching its peak value, and the cut-off frequency ($f_{\mathrm{T}}/f_{\mathrm{MAX}}$) follows a similar trend as G_{m}. This phenomenon can result in significant signal distortion at the device level [3]. Therefore, it becomes crucial to mitigate the rapid decrease in G_{m} at high drain current.

In recent years, GaN-based HEMTs with nanowire channel structure (NC-HEMTs) have been proposed to enhance the linearity of G_{m} [4, 5]. The modulation of the electric field from three directions by the gate electrode effectively suppresses the increase of R_{S} with the rising drain current. However, the presence of a stronger depletion effect of the three-dimensional gate leads to a rapid pinching off of the two-dimensional electron gas (2DEG) channel. In addition, at a higher V_{GS}, the stronger longitudinal electric field still makes G_{m} drop off [4]. Hence, the further improvement of linearity is limited by NC-HEMTs.

Based on the aforementioned, a top-MIS-gate (metal-insulator-semiconductor gate) NC-HEMT (TMGNC-HEMT) for linearity enhancement is introduced in this study. Compared with the traditional NC-HEMTs [4], the TMGNC-HEMT has a top-MIS-gate instead of a Top-Schottky-gate. Due to the weakened control of the Top-MIS gate by the in-situ SiN under its top-gate metal, the electron in the nanowire channel is gradually depleted by the lateral sidewall gate. Therefore, the linearity of G_{m} and the linearity of $f_{\mathrm{T}}/f_{\mathrm{MAX}}$ are enhanced by the TMGNC-HEMT. In addition, the proposed device achieves a saturated power density (P_{sat}) of 3.2 W/mm with a 1-dB compression point (P_{1dB}) of 25.1 dBm at V_{DS} of 18 V. The power-added-efficiency (PAE) at P_{1dB} reaches 63.5%, closely approaching the peak PAE of 63.6%. In addition, a new perspective is introduced, analyzing the improved linearity of the TMGNC-HEMT through the variation in electron concentration distribution with the increase of negative V_{GS}.

Experiment. The epitaxial layers of heterojunction were grown by metal-organic chemical vapor deposition on a SiC substrate. For more details on device fabrication, please see Appendix A.

Results and discussion. Compared with the TMGNC-HEMT, the off-state current characteristic of the MIS-planar-HEMT degenerates significantly in Figure 1(h). To investigate the reason, the distribution of electron concentration changing with VGS of the TMGNC-HEMT and the MIS-planar-HEMT is simulated in Figure 1(j). For MIS-planar-HEMT, due to the absence of lateral depletion, the channel cannot be effectively pitched off. However, for TMGNC-HEMT, the electron in the nanowire channel is gradually depleted by both the top gate and the additional lateral gate, but the lateral gate mainly controls the channel.

As shown in Figure 1(i), the I_{DS} of NC-HEMT decreases to 856 mA/mm due to the removal of the partial barrier by etching. Attributed to stress-engineered in-situ SiN technology, the piezoelectric polarization of the AlGaN barrier is enhanced [6]. The I_{DS} of the TMGNC-HEMT exceeds that of planar-HEMT (i.e., I_{DS} of 1039 mA/mm), reaching 1198 mA/mm. In Figure 1(k), the dynamic source access resistance was obtained by the gate current injection method [7]. The constant normalized source access resistance ($R_{\mathrm{S}}/R_{\mathrm{S0}}$) indicates that the TMGNC-HEMT exhibits excellent current drivability in the source access region, which makes the G_{m} drop slowly with the increasing drain current. As shown in Figure 1(l), for TMGNC-HEMT, even at high drain current levels, G_{m} does not exhibit a sig-

* Corresponding author (email: miminhan@qq.com)

© Science China Press 2025

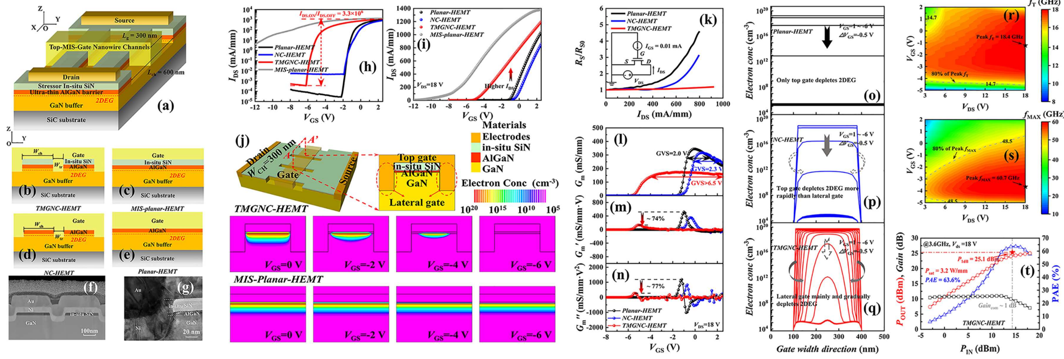

Figure 1 (Color online) (a) Schematic diagram of TMGNC-HEMT. (b)–(e) Cross-sectional diagrams of four kinds of HEMTs. (f) SEM image of the TMGNC structure. (g) HRTEM image of one side of the TMGNC structure. Comparison of $I_{\rm DS}$-$V_{\rm GS}$ characteristics in (h) the log coordinate and (i) linear coordinate of the four kinds of HEMTs at $V_{\rm DS}$ of 18 V. (j) Simulation on the electron concentration distribution for the TMGNC-HEMT and the MIS-planar-HEMT when $V_{\rm GS}$ drops from 0 to −6 V. (k) Normalized $R_{\rm S}/R_{\rm S0}$ of planar-HEMT, NC-HEMT, and TMGNC-HEMT. Comparison of (l) $G_{\rm m}$, (m) $G'_{\rm m}$, and (n) $G''_{\rm m}$ characteristics of the planar-HEMT, NC-HEMT, and TMGNC-HEMT. The electron concentration varies with $V_{\rm GS}$ decreasing from 1 to −6 V for (o) planar-HEMT, (p) NC-HEMT, and (q) TMGNC-HEMT at the 2DEG channel position along the gate width direction. The variations in (r) $f_{\rm T}$ and (s) $f_{\rm MAX}$ as a function of the $V_{\rm GS}$ and $V_{\rm DS}$ of TMGNC-HEMT. The peak $f_{\rm T}$ and the peak $f_{\rm MAX}$ are 18.4 and 60.7 GHz, respectively. (t) Load-pull measurement at $V_{\rm DS}$ of 18 V for TMGNC-HEMT at 3.6 GHz.

nificant decrease, and the gate-voltage-swing (GVS) exceeds 6.5 V, which is about 3.25 times as high as that of a planar-HEMT. In addition, the first derivative and second derivative ($G'_{\rm m}$ and $G''_{\rm m}$) of the $G_{\rm m}$ are shown in Figures 1(m) and (n). Notably, both the $G'_{\rm m}$ and $G''_{\rm m}$ of the TMGNC-HEMT are lowest compared with those of planar-HEMT and NC-HEMT, which will result in good gain linearity. The reason for the improvement of linearity of $G_{\rm m}$ is further analyzed by TCAD simulation. For planar-HEMT, NC-HEMT, and TMGNC-HEMT, the curves of electron concentration varying with decreasing $V_{\rm GS}$ at the 2DEG channel position along the gate width direction are extracted in Figures 1(o)–(q). For planar-HEMT and NC-HEMT, the depletion effect of the top gate is too strong, resulting in a rapid decline in $G_{\rm m}$. However, for TMGNC-HEMT, benefiting from the suppression of top-gated depletion by the in-situ SiN, the control ability of the top gate on the channel is weakened, such that the lateral gate mainly controls the channel and gradually pinches off the channel with the increase of negative $V_{\rm GS}$. Therefore, the $G_{\rm m}$ of TMGNC-HEMT is broadened and flat.

The variations in $f_{\rm T}$ and $f_{\rm MAX}$ as a function of $V_{\rm GS}$ and $V_{\rm DS}$ are displayed in Figures 1(r) and (s). When the cut-off frequencies are reduced to 80% of the peaks, $f_{\rm T}$ and $f_{\rm MAX}$ are selected to be 14.7 and 48.5 GHz, respectively. Therefore, the wide range selected by the gray solid lines indicates that the TMGNC-HEMT has a decent linearity of cut-off frequencies. At $V_{\rm DS}$ of 18 V, the GVS of $f_{\rm T}$ and $f_{\rm MAX}$ can reach 6.6 and 5.6 V, respectively. Thus, the flat cut-off frequency profiles of the TMGNC-HEMT reflect uniform power gain within the wide voltage ranges. The continuous-wave radio frequency (RF) power characteristics of TMGNC-HEMT were measured at 3.6 GHz at $V_{\rm DS}$ of 18 V, as shown in Figure 1(t). Owing to the flat power gain, the TMGNC-HEMT obtained a saturated power density $P_{\rm sat}$ of 3.2 W/mm with the associated 1-dB compression point ($P_{\rm 1dB}$) of 25.1 dBm at $V_{\rm DS}$ of 18 V. When the linear power gain is compressed by 1 dB, the PAE of the TMGNC-HEMT reaches 63.5%. The results of the RF power measurement illustrate that the TMGNC-HEMT can meet the requirements of sufficient output power, high efficiency, and decent linear transmission in communication applications.

Conclusion. The linearity of $G_{\rm m}$ and the linearity of $f_{\rm T}/f_{\rm MAX}$ are enhanced by the proposed TMGNC-HEMT. This improvement can be attributed to the in-situ SiN cap, which effectively suppresses top-gated depletion, ensuring the gradual depletion of the lateral gate. Therefore, the GVS of $G_{\rm m}$ can exceed 6.5 V with the low $G'_{\rm m}$ and $G''_{\rm m}$ for TMGNC-HEMT. In addition, the $f_{\rm T}$ and $f_{\rm MAX}$ of the TMGNC-HEMT remain almost unchanged across a broad range of $V_{\rm GS}$ and $V_{\rm DS}$. Significantly benefiting from the gradual gain compression, the device achieves a PAE of 63.5% at the 1-dB gain compression point and a $P_{\rm sat}$ of 3.2 W/mm at 3.6 GHz.

Acknowledgements This work was supported by National Key Research and Development Project of China (Grant No. 2023YFB3609604), Key R&D Program of Guangzhou (Grant No. 202103020002), Fundamental Research Funds for the Central Universities (Grant No. YJSJ24020), and ZTE Industry-University-Institute Cooperation Funds (Grant No. HC-CN-20220708005).

Supporting information Appendixes A–C. The supporting information is available online at info.scichina.com and link.springer.com. The supporting materials are published as submitted, without typesetting or editing. The responsibility for scientific accuracy and content remains entirely with the authors.

References

1 Nakajima S. GaN HEMTs for 5G base station applications. In: Proceedings of IEEE International Electron Devices Meeting (IEDM), San Francisco, 2018
2 Yu Q, Then H W, Thomson D, et al. 5G mmWave power amplifier and low-noise amplifier in 300 mm GaN-on-Si technology. In: Proceedings of IEEE Symposium on VLSI Technology and Circuits, Honolulu, 2022. 126–127
3 Joglekar S, Radhakrishna U, Piedra D, et al. Large signal linearity enhancement of AlGaN/GaN high electron mobility transistors by device-level Vt engineering for transconductance compensation. In: Proceedings of IEEE International Electron Devices Meeting (IEDM), San Francisco, 2017
4 Zhang K, Kong Y, Zhu G, et al. High-linearity AlGaN/GaN FinFETs for microwave power applications. IEEE Electron Device Lett, 2017, 38: 615–618
5 Xing W, Liu Z, Qiu H, et al. Planar-nanostrip-channel InAlN/GaN HEMTs on Si with improved g_m and f_T linearity. IEEE Electron Device Lett, 2017, 38: 619–622
6 Wu S, Mi M, Zhang M, et al. A high RF-performance AlGaN/GaN HEMT with ultrathin barrier and stressor in situ SiN. IEEE Trans Electron Devices, 2021, 68: 5553–5558
7 Palacios T, Rajan S, Chakraborty A, et al. Influence of the dynamic access resistance in the g_m and f_T linearity of AlGaN/GaN HEMTs. IEEE Trans Electron Devices, 2005, 52: 2117–2123